Cisplatin overcomes Bcl-2-mediated resistance to apoptosis via preferential engagement of Bak: critical role of Noxa-mediated lipid peroxidation

Ozgur Kutuk[1], Elif Damla Arisan[1], Tugsan Tezil[1], Maria C.Shoshan[2] and Huveyda Basaga[1,*]

[1]Biological Sciences and Bioengineering Program, Sabanci University, 34956 Tuzla, Istanbul, Turkey and [2]Department of Oncology-Pathology, CCK R8:03, Karolinska Institute, S-17176 Stockholm, Sweden

*To whom correspondence should be addressed. Tel: +90 216 483 9511; Fax: +90 216 483 9550;
Email: huveyda@sabanciuniv.edu

Increased expression of antiapoptotic Bcl-2 proteins confers therapeutic resistance in various cancer types. Targeting Bcl-2 proteins by small molecules or activating alternative pathways to bypass Bcl-2-mediated protection to promote apoptosis are two approaches to overcoming therapeutic resistance. Here, we show that cisplatin triggers a Bak-dependent pathway to induce apoptosis in Bcl-2-overexpressing MCF-7 cells. p53-mediated induction of Noxa expression, generation of lipid peroxidation end products and induction of Noxa–Mcl-1 interaction are necessary for this pathway to function. Although Puma is also induced by cisplatin treatment, it is not required for apoptosis. Similarly, reactive oxygen species production by cisplatin did not have any effect on cisplatin-induced apoptosis in MCF-7 Bcl-2 cells. Furthermore, p53 promotes cisplatin-induced apoptosis by directly binding and counteracting Bcl-x_L antiapoptotic function. In conclusion, our findings suggest a novel mode of action for cisplatin to overcome Bcl-2-mediated protection against apoptosis, which requires preferential activation of Bak and p53-mediated upregulation of Noxa protein levels and lipid peroxidation.

Introduction

Several studies have shown that expression of Bcl-2 confers resistance to apoptosis insults including chemotherapeutics (1–5). Intrinsic or mitochondrial apoptotic pathway is regulated mainly by protein–protein interactions of Bcl-2 protein family members. Briefly, activation and oligomerization of proapoptotic multidomain Bax and Bak triggers mitochondrial outer membrane permeabilization, which is followed by the release of cytochrome *c* into cytosol. When cytochrome *c* translocates into cytosol, it promotes the activation of caspase-9 by a mechanism involving formation of apoptosome complex with Apaf-1 and procaspase-9 (6).

Antiapoptotic Bcl-2 proteins (Bcl-2, Bcl-x_L, Mcl-1, Bcl-w, Bfl-1/A1) interfere with engagement of mitochondrial apoptotic machinery by inhibiting oligomerization of Bax and Bak. To exert this antiapoptotic function, they either directly sequester Bax and Bak to prevent their oligomerization or sequester activator BH3-only proteins, including Bid and Bim, to block the activation of Bax and Bak (7,8). Following the transduction of a proapoptotic signal, sensitizer BH3-only proteins (Bad, Bmf, Puma, Noxa, Hrk, Bik) displace Bax and Bak or activator BH3-only proteins from their antiapoptotic guardians to promote cell death (7,9,10). Moreover, it has been recently shown that BH3-only proteins selectively interact with antiapoptotic Bcl-2 proteins (11). For example, Noxa exhibits a high affinity for Mcl-1 and not Bcl-2 or Bcl-x_L, whereas Bim interacts with all three antiapoptotic proteins.

Oxidative alteration of biological membranes or lipoproteins may generate a spectrum of lipid peroxidation end products which may lead to modification of proteins. For instance, lipoxygenases and cyclooxygenases catalyze the stereospecific insertion of molecular oxygen to polyunsaturated fatty acids and formation of prostaglandins and leukotrienes. Post-translational modification of cellular proteins by reactive lipid products and induction of apoptosis by lipid peroxidation end products has been shown to play an important role in the pathogenesis of various human pathologies involving atherosclerosis, diabetes and neurodegenerative disorders (12). Activation of upstream prodeath signaling pathways such as stress kinases c-jun N-terminal kinase and p38 by lipid peroxidation end products was demonstrated to trigger mitochondrial apoptotic pathway (13,14). In addition to its direct prosurvival effect on mitochondria via protein–protein interaction, Bcl-2 was shown to inhibit lipid peroxidation and reactive oxygen species (ROS) production, but the significance of this function of Bcl-2 is not well understood (15–17).

Cisplatin is a commonly used DNA-damaging drug in the treatment of a variety of human malignancies. A p53-dependent apoptotic pathway or cell cycle arrest or p53-independent apoptosis have all been suggested to be involved in the anticancer effect of cisplatin (18–22). Evidently, the downstream effectors of cisplatin-induced p53-mediated apoptosis remain incompletely defined. An added complexity of p53-mediated apoptosis model is that p53 was reported to translocate to mitochondria and interact with Bcl-2 protein family members to promote transcription-independent apoptosis (23–27).

Here, we report that cisplatin treatment overcomes Bcl-2-mediated protection in MCF-7 cells (wt p53), but not in MDA-MB-231 cells (mt p53), whereas a taxane (paclitaxel) or a small-molecule Bcl-2 inhibitor (HA14-1) failed to act similarly. We also find that p53-dependent Noxa upregulation and lipid peroxidation is essential in this process. Additionally, Noxa upregulation is accompanied by increased Noxa/Mcl-1 and reduced Bak–Mcl-1 complexes, which triggers the activation of Bak, but not Bax. In addition to its transcription-dependent proapoptotic function, p53 potentiates cisplatin-induced apoptosis by directly binding and neutralizing Bcl-x_L. Overall, our data suggest a novel mode of action for cisplatin to overcome Bcl-2-mediated protection against apoptosis, which requires preferential engagement of Bak-dependent mitochondrial apoptotic pathway.

Material and methods

Cell lines

MCF-7 and MDA-MB-231 breast cancer cell lines were grown in RPMI 1640 and Dulbecco's modified Eagle's medium (Biological Industries, Beit-Haemek, Israel) with 2 mM L-glutamine, 10% fetal calf serum, 100 IU/ml penicillin and 100 μg/ml streptomycin in a humidified incubator at 37°C and 5% CO_2. For stable transfection of MCF-7 and MDA-MB-231, cells were transfected with pcDNA3 Bcl-2 plasmid (Addgene plasmid 8768) (28), using Fugene 6 (Roche, Mannheim, Germany) and clonal selection was carried out using G418 (Sigma, St Louis, MO). Selected clones were verified by immunoblot analysis of Bcl-2 and maintained in growth medium with 0.25 mg/ml G418. MCF-7 Bcl-2 cells were grown to 50% confluency and transiently transfected with pCMV empty vector (Vector) or pCMV-p53DD (plasmid encoding a dominant-negative p53 lacking DNA-binding domain; kindly provided by Moshe Oren, Weizmann Institute of Science) (29), using Fugene 6 (Roche) for 16 h before treatments. Expression of p53DD (14 kDa) was confirmed by immunoblotting using a pan-p53 antibody (pAB421; Calbiochem, San Diego, CA).

Chemicals

Bcl-2 inhibitor HA14-1 [Ethyl-2-amino-6-bromo-4-(lcyano-2-ethoxy-2-oxoethyl)-4H-chromene-3-carboxylate] was purchased from Calbiochem. Solutions of HA14-1 were freshly prepared before each experiment (dissolved in dimethyl sulfoxide as 5 mM stock solution). Cisplatin, paclitaxel, N-acetyl-L-cysteine, 2,2,6,6-tetramethylpiperidinyloxy, Tiron and dichlorofluorescein diacetate (DCF-DA) were purchased from Sigma. Trolox and U-74389G were from Calbiochem. C_{11}-BODIPY (581/591) and MitoTracker Red CMXRos were purchased from Molecular Probes (Invitrogen, Carlsbad, CA).

Abbreviations: ELISA, enzyme-linked immunosorbent assay; MMP, mitochondrial membrane potential; PCR, polymerase chain reaction; ROS, reactive oxygen species; RT, reverse transcription; siRNA, small interfering RNA; 4-HNE, 4-hydroxynonenal.

O.Kutuk *et al.*

Apoptosis assays

Apoptosis was assessed by quantifying the exposure of phosphatidylserine using Annexin V-fluorescein isothiocyanate (Roche). Briefly, cells were treated as described in the figure legends, incubated in binding buffer for 10 min and analyzed by flow cytometry. Accumulated DEVDase activity was assessed as levels of specifically DEVDase-cleaved cytokeratin-18 (CK18) in total cell lysates using M30 Apoptosense enzyme-linked immunosorbent assay (ELISA) (PEVIVA AB, Bromma, Sweden) (30). MCF-7 and MDA-MB-231 breast cancer cell lines were seeded in 96-well plates and treated as indicated. M30 ELISA plate was assayed according to the manufacturer's instructions and the concentration of M30 antigen, indicating cleaved CK18, is presented as fold increase in units per liter.

Detection of ROS and lipid peroxidation

ROS produced by different drugs was determined using the oxidation-sensitive probe DCF-DA as described before on a Spectramax Gemini Fluorometer plate reader (31). The extent of lipid peroxidation in untreated and drug-exposed samples was determined by measuring the thiobarbituric acid reactive substance as described before (32). Lipid peroxidation was also evaluated using C_{11}-BODIPY (581/591) as described previously (33). Cells were incubated with C_{11}-BODIPY (581/591) 30 min before measurements. C_{11}-BODIPY (581/591) fluorescence was analyzed both at 485 nm excitation/460 nm emission and 535 nm excitation/615 nm emission to measure its oxidized and reduced forms on a multiplate fluorometer. Data are expressed as C11-Bodipy Green (oxidized)/total ratio.

Real-time quantitative polymerase chain reaction

Total RNA was isolated using a TRIzol reagent (Invitrogen) following the procedure described by the manufacturer. Reverse transcription (RT) was performed using a specific RT kit (Qiagen, Hilden, Germany). The RT reaction mixture contained 1 µg of total RNA, 500 ng of oligo(dT) primer, 5× RT reaction buffer, 10 mM deoxynucleoside triphosphates and 200 U of a reverse transcriptase (Qiagen) in a total volume of 20 µl. Then, all samples were incubated in 37°C for 1 h. The quantity of cDNA was calculated using spectrophotometry by determination of optical density at 260 nm. Purity was calculated using $OD_{260/280}$ ratio. Real-time quantitative polymerase chain reaction (PCR) was performed in 96-well 0.2 ml thin wall PCR plates using the iCycler Thermal Cycler (Bio-Rad, Hercules, CA) and carried out with QuantiTect SYBR Green PCR Master Mix (Qiagen), which contains HotStarTaq DNA Polymerase, QuantiTect SYBR Green PCR Buffer and SYBR Green I. The real-time PCR mixture contained 1× QuantiTect SYBR Green PCR Master Mix, 0.3 µM primer pairs and 500 ng cDNA in a total volume of 25 µl. Specific primers were from Qiagen; Hs_PMAIP1_1_SG QuantiTect Primer Assay for Noxa and Hs_BBC3_1_SG QuantiTect Primer Assay for Puma. The mixture was heated initially at 95°C for 15 min in order to activate HotStarTaq DNA Polymerase and then followed by 40 cycles with denaturation at 94°C for 1 min, annealing at 50–54°C for 1 min and extension at 72°C for 1 min. Furthermore, the generation of amplified products was identified by melting curve analysis. The melt curve protocols designed for increment temperatures of 0.5°C with a starting temperature of 45°C and ending at 90°C were repeated to ensure that primer dimers and other non-specific products had been minimized or eliminated. Data were analyzed using iCycler IQ software with all samples normalized to the 18 S ribosomal RNA.

Immunoblot analysis

Cells were treated with drugs as indicated before and total cell lysates were prepared in 20 mM Tris–HCl (pH 7.5), 150 mM NaCl, NP-40 0.5%, (vol/vol), 1 mM ethylenediaminetetraacetic acid, 0.5 mM phenylmethylsulfonyl fluoride, 1 mM dithiothreitol, protease inhibitor cocktail (Roche). Proteins were separated on sodium dodecyl sulfate–polyacrylamide gel electrophoresis and transferred onto polyvinylidene difluoride membranes (GE Healthcare, Little Chalfont, UK). Membranes were then blocked with 5% milk blocking solution in Tris-buffered saline-Tween 20 and incubated with appropriate primary and horseradish peroxidase-conjugated secondary antibodies in the buffer containing 5% (vol/vol) milk blocking solution. Proteins were finally analyzed using an enhanced chemiluminescence detection system enhanced chemiluminescence Advance (GE Healthcare) and exposed to Hyperfilm enhanced chemiluminescence (GE Healthcare). The following antibodies were used for immunoblotting: anti-Bcl-2 (#2872), anti-Bcl-x_L (#2762), anti-Mcl-1 (#4572), anti-Puma (#4976), anti-Bax (#2774), anti-Bak (#3814), anti-β-Actin (#4967), anti-caspase-9 (#9501) (Cell Signaling, Beverly, MA), anti-Noxa (114C307; Calbiochem), p53 (DO-1; Santa Cruz Biotechnology, Santa Cruz, CA), p53 (pAB421; Calbiochem), anti-cytochrome *c* (6H2.B4; BD Biosciences, San Jose, CA), anti-CoxIV (A21347; Molecular Probes, Carlsbad, CA). Anti-HNE monoclonal antibody specific for the 4-hydroxynonenal (4-HNE) histidine adduct was kindly provided by Koji Uchida (Graduate School of Bioagricultural Sciences, Nagoya University) (34).

Subcellular fractionation

Subcellular fractionation was performed as described before (35). Mitochondria-enriched pellet and cytosolic supernatant fractions were used to monitor cytochrome *c* release from mitochondria by means of immunoblot analysis.

Small interfering RNA transfection

MCF-7 cells were transfected with Bcl-2 small interfering RNA (siRNA) and MCF-7 BCL-2 cells were transfected with Bcl-2 siRNA (Hs_BCL2_9 HP Validated siRNA; Qiagen), p53 siRNA (Hs_TP53_9 HP Validated siRNA; Qiagen), Puma siRNA (Hs_BBC3_2 HP Validated siRNA; Qiagen) and Noxa siRNA (Hs_PMAIP1_5 HP siRNA; Qiagen) by using Hiperfect transfection reagent (Qiagen) according to the manufacturer's instructions. Cells were also transfected with negative control (scramble) siRNA (Negative Control siRNA; Qiagen) to monitor off target effects. The efficiency of protein knockdown was verified by immunoblotting after 48 h of transfection.

Coimmunoprecipitation

Cell lysates were isolated in 1% Chaps buffer [5 mM $MgCl_2$, 137 mM NaCl, 1 mM ethylenediaminetetraacetic acid, 1 mM EGTA, 1% Chaps, 20 mM Tris–HCl (pH 7.5) and protease inhibitors (Roche)] as described previously (27). Proteins (1200 µg) were immunoprecipitated with anti-Bcl-2 (#2872), anti-Bcl-x_L (#2762), anti-Mcl-1 (#4572) from Cell Signaling and p53 (DO-1; Santa Cruz), anti-Noxa (114C307; Calbiochem) at 4°C for 2 h or overnight. Immunoprecipitates were captured by 50% slurry of protein G-Sepharose (GE Healthcare) in lysis buffer at 4°C for 2 h. Immunoprecipitates were then recovered by centrifugation and washed three times in 1% Chaps buffer. The samples were subsequently analyzed by immunoblot to detect interacting proteins.

Caspase activation assays

The activity of caspase-9 was determined by ApoAlert Caspase-9/6 Fluorescent Assay Kit (Clontech, Palo Alto, CA) according to the manufacturer's protocol. The release of fluorochrome 7-amino-4-methylcoumarin was analyzed at 380 nm excitation and 460 nm emission using a multiplate fluorometer. Results are derived as mean ± SE of three independent experiments in duplicate and expressed in arbitrary fluorescence units per mg of protein. Data are shown as fold increase over control.

Assessment of Bax and Bak activation

Cells were lysed in 1% Chaps buffer and activation of Bax and Bak was evaluated by immunoprecipitation using active conformation-specific antibodies anti-Bax (6A7; BD Pharmingen, San Diego, CA) and anti-Bak (Ab-2; Calbiochem) and the immunoprecipitated proteins were detected by immunoblot analysis. Detection of Bax and Bak activation by intracellular staining and flow cytometry using active conformation-specific antibodies anti-Bax (6A7; BD Pharmingen) and anti-Bak (Ab-1; Calbiochem) was performed as described previously (36). Activation of Bax or Bak was determined by a shift to the right in the histogram.

Measurement of mitochondrial membrane potential

The loss of mitochondrial membrane potential (MMP) was evaluated as described previously using MitoTracker Red CMXRos (37). The percentage of MMP loss corresponds to the percentage of cells with low MMP.

Statistical analysis

Statistical significance of the results was analyzed using Student's *t*-tail test using GraphPad Prism software. $P < 0.05$ and $P < 0.01$ were considered significant.

Results

Cisplatin activates mitochondrial apoptosis in Bcl-2-overexpressing MCF-7 cells

Since Bcl-2 is known to protect against various apoptotic insult including chemotherapeutic drugs, we initially evaluated how Bcl-2 overexpression alters apoptotic response induced by three drugs with different mechanism of action: a microtubule-damaging taxane (paclitaxel), a DNA-damaging platinum agent (cisplatin) and a small-molecule Bcl-2 inhibitor (HA14-1). In MCF-7 and MDA-MB-231 cells, paclitaxel, cisplatin or HA14-1 significantly induced apoptosis after 24 and 48 h of treatment. MCF-7 and MDA-MB-231 cells were stably transfected with Bcl-2 and the expression level of Bcl-2 in parental and Bcl-2-transfected cells was verified by using immunoblotting (supplementary Figure S1A is available at

Carcinogenesis Online). As shown in Figure 1A, overexpression of Bcl-2 protected against apoptosis triggered by paclitaxel, cisplatin or HA14-1 following treatment for 24 h in both MCF-7 Bcl-2 and MDA-MB-231 Bcl-2 cells. This protective potency of Bcl-2 was observed still after 48 h treatment in MDA-MB-231 Bcl-2 cells. Although Bcl-2 expression decreased paclitaxel- and HA14-1-induced apoptosis following 48 h treatment in MCF-7 Bcl-2 cells, cisplatin was able to trigger apoptosis as determined by Annexin V staining (Figure 1A). Activation of apoptosis by cisplatin in MCF-7 Bcl-2 cells was also confirmed by M30 Apoptosense assay (supplementary Figure S1B is available at *Carcinogenesis* Online). In addition, cisplatin treatment for 48 h led to mitochondrial release of cytochrome *c* into cytosol and loss of MMP in MCF-7 Bcl-2 cells (Figure 1B and C), even though paclitaxel or HA14-1 did not elicit similar effects. Treatment with cisplatin, paclitaxel or HA14-1 caused loss of MMP in MDA-MB-231 cells. In contrast, they did not lead to loss of MMP in Bcl-2-overexpressing MDA-MB-231 cells after treatment for 48 h (Figure 1C). Furthermore, exposure of MCF-7 Bcl-2 cells to cisplatin, but not to paclitaxel or HA14-1 resulted in activation of caspase-9, whereas all three drugs induced activation of caspase-9 in parental MCF-7 cells (Figure 1D). Treatment of MDA-MB-231 cells with cisplatin, paclitaxel or HA14-1 resulted in activation of caspase-9 and overexpression of Bcl-2 decreased caspase-9 activation by all three drugs in MDA-MB-231 Bcl-2 cells (Figure 1D). Taken together, these results show that cisplatin treatment overcomes Bcl-2-mediated resistance to apoptosis in MCF-7 Bcl-2 cells via promoting mitochondrial apoptotic signaling.

*Cisplatin activates Bak, not Bax in Bcl-2-overexpressing MCF-7 cells*

The multidomain proapoptotic Bcl-2 proteins Bax and Bak are activated upon apoptotic stimuli to facilitate the permeabilization of mitochondrial outer membrane and cytochrome *c* release into cytosol. To explore the activation of Bax or Bak in MCF-7 Bcl-2 treated with cisplatin for 36 h, we immunoprecipitated Bak and Bak using conformation-specific antibodies which recognize their exposed N-terminal epitopes. Whereas both Bax and Bak were activated by cisplatin in MCF-7 cells following treatment with cisplatin, Bak, but not Bax, was activated in MCF-7 Bcl-2 cells (Figure 2A). Moreover, we confirmed these results by analyzing active Bax and active Bak by means of immunofluorescence staining and flow cytometry detection (Figure 2B). However, activation of Bax and Bak by cisplatin in MDA-MB-231 cells was completely blocked in MDA-MB-231 Bcl-2 cells (Figure 2A). These results suggest that cisplatin treatment triggers a preferential activation of Bak-mediated apoptosis pathway in MCF-7 Bcl-2 cells, even though Bcl-2 overexpression decreases Bax activation.

Increased lipid peroxidation accompanies cisplatin-induced apoptosis in MCF-7 Bcl-2 cells

To establish the role of Bcl-2 in the apoptotic response, ROS production and lipid peroxidation in MCF-7 cells, we performed knockdown experiments with Bcl-2 siRNA and scramble siRNA. We transfected MCF-7 cells with Bcl-2 siRNA and monitored the formation of apoptotic response, ROS formation and lipid
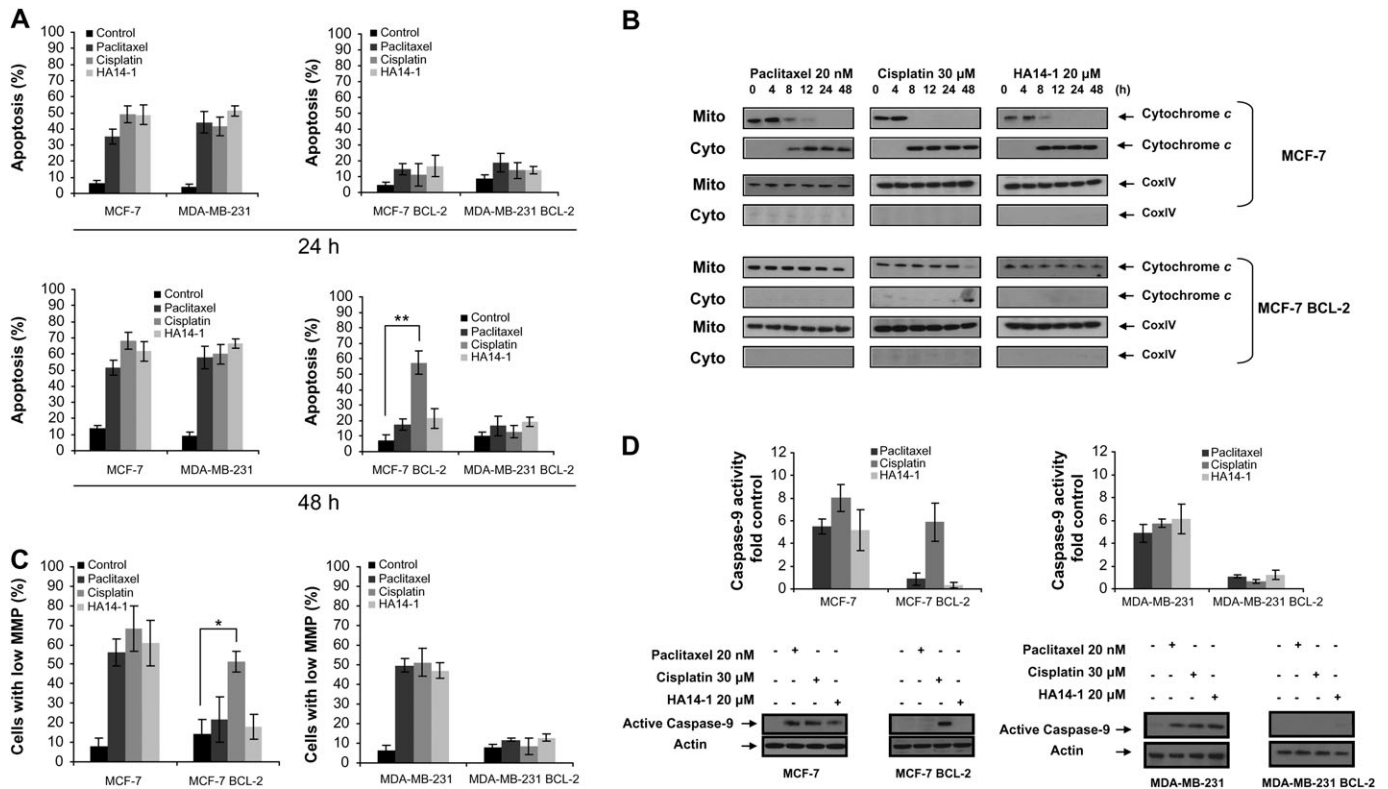
Fig. 1. Cisplatin but not paclitaxel or HA14-1 induces apoptosis in MCF-7 Bcl-2 cells. (**A**) MCF-7, MCF-7 Bcl-2, MDA-MB-231 and MDA-MB-231 Bcl-2 cells were treated with paclitaxel (20 nM), cisplatin (30 μM) and HA14-1 (20 μM) for 24 (top) or 48 h (bottom) and apoptosis was evaluated by Annexin V staining. Columns, mean of three independent experiments; bars, standard error. $^{**}P < 0.01$, cisplatin-treated compared with untreated control cells. (**B**) MCF-7 and MCF-7 Bcl-2 cells were treated with paclitaxel (20 nM), cisplatin (30 μM) and HA14-1 (20 μM) for 0–48 h. Cytosolic and mitochondrial fractions were probed for cytochrome *c* by immunoblotting. CoxIV was used as a loading control for mitochondrial fractions. (**C**) MCF-7, MCF-7 Bcl-2, MDA-MB-231 and MDA-MB-231 Bcl-2 cells were treated with paclitaxel (20 nM), cisplatin (30 μM) and HA14-1 (20 μM) for 48 h and % of cells with low MMP was detected by flow cytometry using MitoTracker Red CMXRos. Columns, mean of three independent experiments; bars, standard error. $^{*}P < 0.05$, cisplatin-treated compared with untreated control cells. (**D**) MCF-7, MCF-7 Bcl-2, MDA-MB-231 and MDA-MB-231 Bcl-2 cells were treated with paclitaxel (20 nM), cisplatin (30 μM) and HA14-1 (20 μM) for 48 h and caspase-9 activation was determined by fluorometric caspase assay (top). Results were shown as fold increase over control. Columns, mean of three independent experiments; bars, standard error. In similar treatment conditions, activation of caspase-9 was also analyzed by immunoblotting using antiactive caspase-9 antibody that recognizes 37 kDa cleaved caspase-9 fragment (bottom). Actin was used as a loading control.
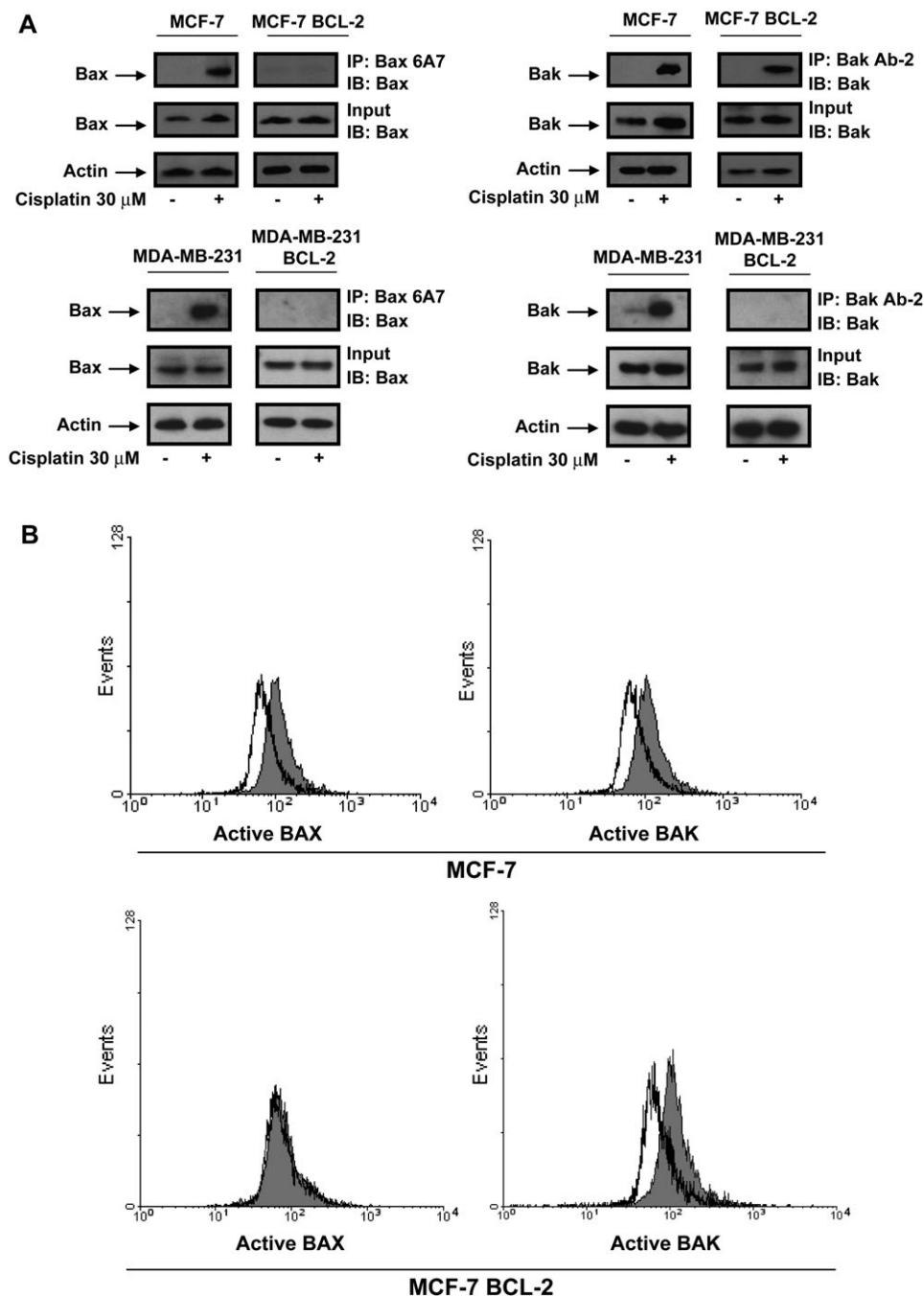
Fig. 2. Cisplatin selectively activates Bak in MCF-7 Bcl-2 cells. (**A**) MCF-7, MCF-7 Bcl-2, MDA-MB-231 and MDA-MB-231 Bcl-2 cells were treated with cisplatin (30 μM) for 36 h. Activation of Bax and Bak was assessed by immunoprecipitation using active conformation-specific anti-Bax (6A7) and anti-Bak (Ab-2) antibodies followed by immunoblot analysis. Five percent of the input for immunoprecipitation was also subjected to immunoblot analysis. Actin was used as a loading control. (**B**) MCF-7 and MCF-7 Bcl-2 cells were treated as in (A), stained for active configuration of Bax (6A7) or Bak (Ab-1), analyzed by fluorescence activated cell sorting for using fluorescein isothiocyanate-labeled secondary antibody for detection. Black line, control cells; gray filled, cisplatin-treated cells.

peroxidation in cells either untreated or treated with cisplatin. The efficiency of knockdown was evaluated by immunoblot analysis of Bcl-2 (Figure 3A). Depletion of Bcl-2 by siRNA did not cause a significant increase in apoptotic response by cisplatin as demonstrated by M30 Apoptosense assay (Figure 3A). Treatment of MCF-7 cells with cisplatin for 24 h significantly increased ROS production compared with untreated cells, but we could not detect a similar effect when cells were treated for 48 h. While knockdown of Bcl-2 in MCF-7 cells led to increased cisplatin-mediated ROS formation after 24 h of treatment, this effect was not observed following 48 h of cisplatin treatment (Figure 3B, left). Bcl-2 siRNA or scramble siRNA alone

did not show any significant effect on ROS formation in MCF-7 cells after 24 or 48 h of treatment. Additionally, pretreatment of MCF-7 cells with scramble siRNA did not effect ROS production by cisplatin.

Cisplatin led to increased lipid peroxidation in MCF-7 cells after 24 and 48 h of treatment as demonstrated by thiobarbituric acid reactive substance formation (Figure 3B, right). Moreover, pretreatment of MCF-7 cells with Bcl-2 siRNA resulted in significantly increased cisplatin-induced lipid peroxidation after 24 and 48 h, although scramble siRNA did not exert such an effect (Figure 3B, right). Of note, Bcl-2 siRNA treatment alone increased lipid peroxidation compared with untreated MCF-7 cells after 48 h, but not after
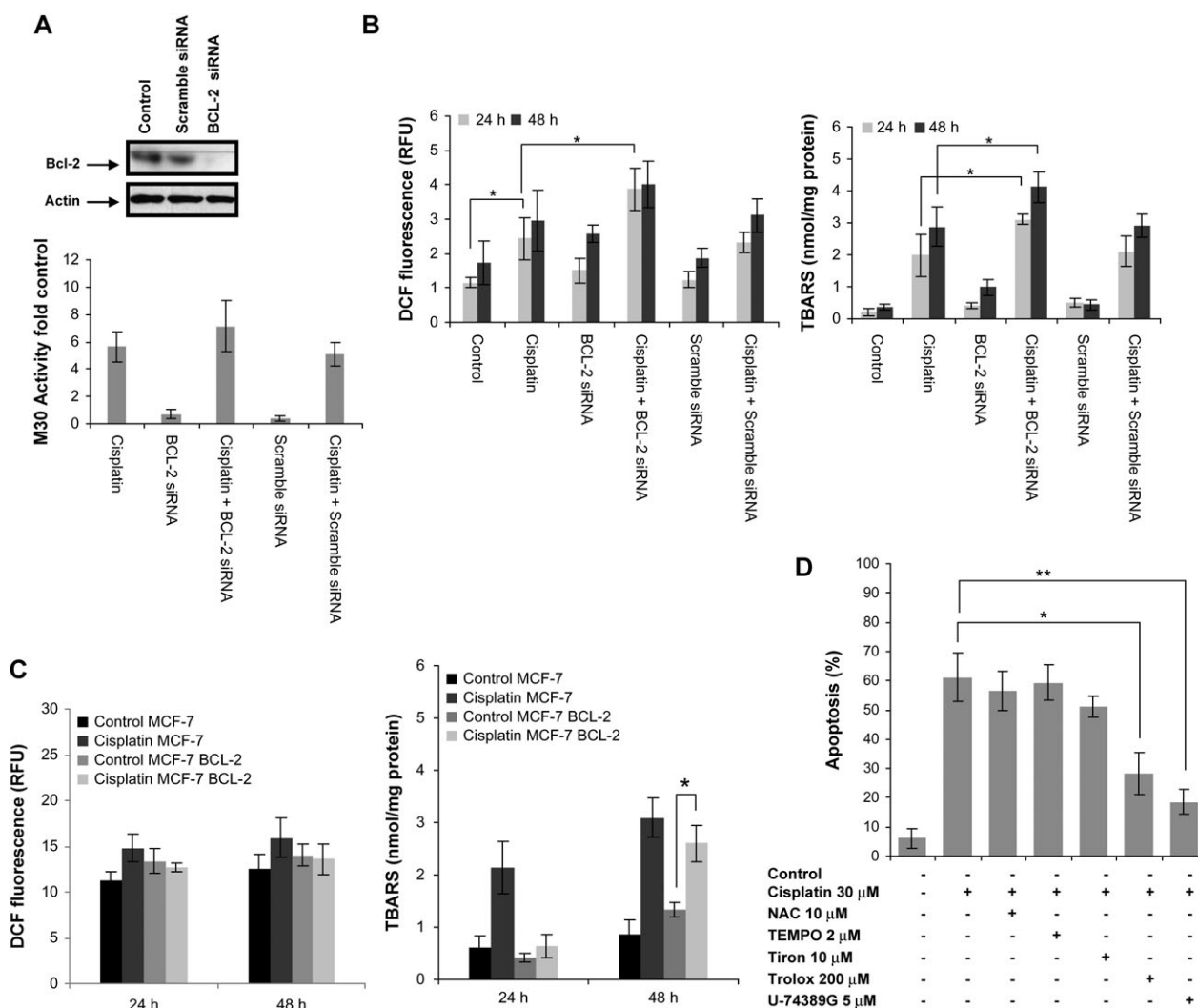
Fig. 3. Lipid peroxidation is involved in cisplatin-induced apoptosis on MCF-7 Bcl-2 cells. (**A**) MCF-7 cells were incubated with Bcl-2 siRNA or scramble siRNA for 48 h. Knockdown of Bcl-2 was verified by immunoblotting. Cells were treated with cisplatin (30 μM) for 48 h and apoptosis was evaluated by M30 Apoptosense assay. Results are shown as fold over control. Columns, mean of three independent experiments; bars, standard error. (**B**) MCF-7 cells were treated with Bcl-2 siRNA or scramble siRNA for 48 h. Both untransfected and siRNA-transfected cells were treated with cisplatin (30 μM) for 24 and 48 h following siRNA transfection and ROS production was determined by using DCF-DA and results were expressed as relative fluorescence units. Columns, mean of three independent experiments; bars, standard error. $^*P < 0.05$, untreated compared with cisplatin-treated cells, cisplatin-treated compared with cisplatin plus Bcl-2 siRNA-treated cells. In addition, lipid peroxidation was assessed by thiobarbituric acid reactive substance (TBARS) measurement and results were expressed as nmol/mg protein. Columns, mean of three independent experiments; bars, standard error. $^*P < 0.05$, cisplatin-treated compared with cisplatin plus Bcl-2 siRNA-treated cells. (**C**) After treatment with cisplatin (30 μM) for 24 and 48 h, MCF-7 and MCF-7 Bcl-2 cells were loaded with DCF-DA and analyzed by multiplate fluorometer. Data were shown as relative fluorescence units (RFU). In parallel, lipid peroxidation in MCF-7 and MCF-7 Bcl-2 cells treated with cisplatin (30 μM) for 24 and 48 h was determined by thiobarbituric acid reactive substance measurement. Results were shown as nmol/mg protein. Columns, mean of three independent experiments; bars, standard error. $^*P < 0.05$, cisplatin-treated compared with untreated control cells. (**D**) MCF-7 Bcl-2 cells with cisplatin (30 μM) or cisplatin plus *N*-acetyl-L-cysteine (NAC) (10 mM), 2,2,6,6-tetramethylpiperidinyloxy (TEMPO) (2 mM), Tiron (10 mM), Trolox (200 μM) or U-74389G (5 μM) for 48 h. Apoptosis was detected by Annexin V staining. Columns, mean of three independent experiments; bars, standard error. $^*P < 0.05$, cisplatin-treated compared with cisplatin plus Trolox-treated cells. $^{**}P < 0.01$, cisplatin-treated compared with cisplatin plus U-74389G-treated cells.

24 h, and scramble siRNA alone did not alter lipid peroxidation in MCF-7 cells.

To test whether ROS production was important for cisplatin-induced apoptosis in MCF-7 Bcl-2 cells, we monitored intracellular ROS formation in MCF-7 and MCF-7 Bcl-2 cells. Exposure of MCF-7 Bcl-2 to cisplatin for 24 or 48 h did not cause any increase in DCF-DA-reactive ROS production compared with untreated control cells, although we observed increased ROS in MCF-7 cells treated with cisplatin for 24 h (Figure 3C). In contrast, cisplatin treatment for 48 h induced increased levels of lipid peroxidation as determined by elevated levels of thiobarbituric acid reactive substance in MCF-7 Bcl-2 cells, although treatment for 24 h did not exert such an effect (Figure 3C). Intriguingly, we observed increased lipid peroxidation in MCF-7 Bcl-2

cells at 48 h compared with 24 h without cisplatin treatment. Cisplatin treatment alone induced lipid peroxidation in MCF-7 cells at both 24 and 48 h of treatment. These data suggest that Bcl-2 expression down-regulates cisplatin-induced ROS production both at 24 and 48 h, but decreases cisplatin-induced lipid peroxidation only at 24 h. We therefore preincubated MCF-7 Bcl-2 cells with antioxidants (*N*-acetyl-L-cysteine, 2,2,6,6-tetramethylpiperidinyloxy, Tiron) and lipid peroxidation inhibitors (Trolox, U-74389G) for 1 h and then treated with cisplatin for 48 h. Apoptotic response was evaluated by Annexin V staining. As demonstrated in Figure 3D, cisplatin-induced apoptosis was decreased by lipid peroxidation inhibitors Trolox and U-74389G, but not by the hydrogen peroxide scavenger *N*-acetyl-L-cysteine and superoxide scavengers 2,2,6,6-tetramethylpiperidinyloxy and Tiron. In

contrast, both ROS scavengers and lipid peroxidation inhibitors decreased cisplatin-induced apoptosis in MCF-7 cells (supplementary Figure S2 is available at *Carcinogenesis* Online). 4-HNE is a highly reactive end product of lipid oxidation of arachidonic acid, linoleic acid or their hydroperoxides (38). We also tested whether Bcl-2 directly scavenges lipid peroxidation end products by using an anti-HNE antibody to detect (4-HNE)-histidine adducts in total cell lysates following Bcl-2 immunoprecipitation. As shown in supplementary Figure S3 (available at *Carcinogenesis* Online), cisplatin treatment for 12 h generated (4-HNE)-histidine adducts in Bcl-2 protein in both MCF-7 and MCF-7 Bcl-2 cells.

In addition, lipid peroxidation inhibitors Trolox and U-74389G decreased cisplatin-induced Bak activation in MCF-7 Bcl-2 cells

(supplementary Figure S4 is available at *Carcinogenesis* Online). Collectively, these data indicate that cisplatin-induced lipid peroxidation but not ROS production is required for cisplatin-induced apoptosis in Bcl-2-overexpressing MCF-7 cells.

Cisplatin induces apoptosis in MCF-7 Bcl-2 cells through upregulation of Noxa

To evaluate the effect of cisplatin treatment on the protein levels of p53, Noxa and Puma in MCF-7 Bcl-2 cells, MCF-7 Bcl-2 cells were treated with cisplatin for 48 h and total protein lysates were analyzed by immunoblotting. As shown in Figure 4A, cisplatin induced increased protein levels of p53, Noxa and Puma in MCF-7 Bcl-2 cells.
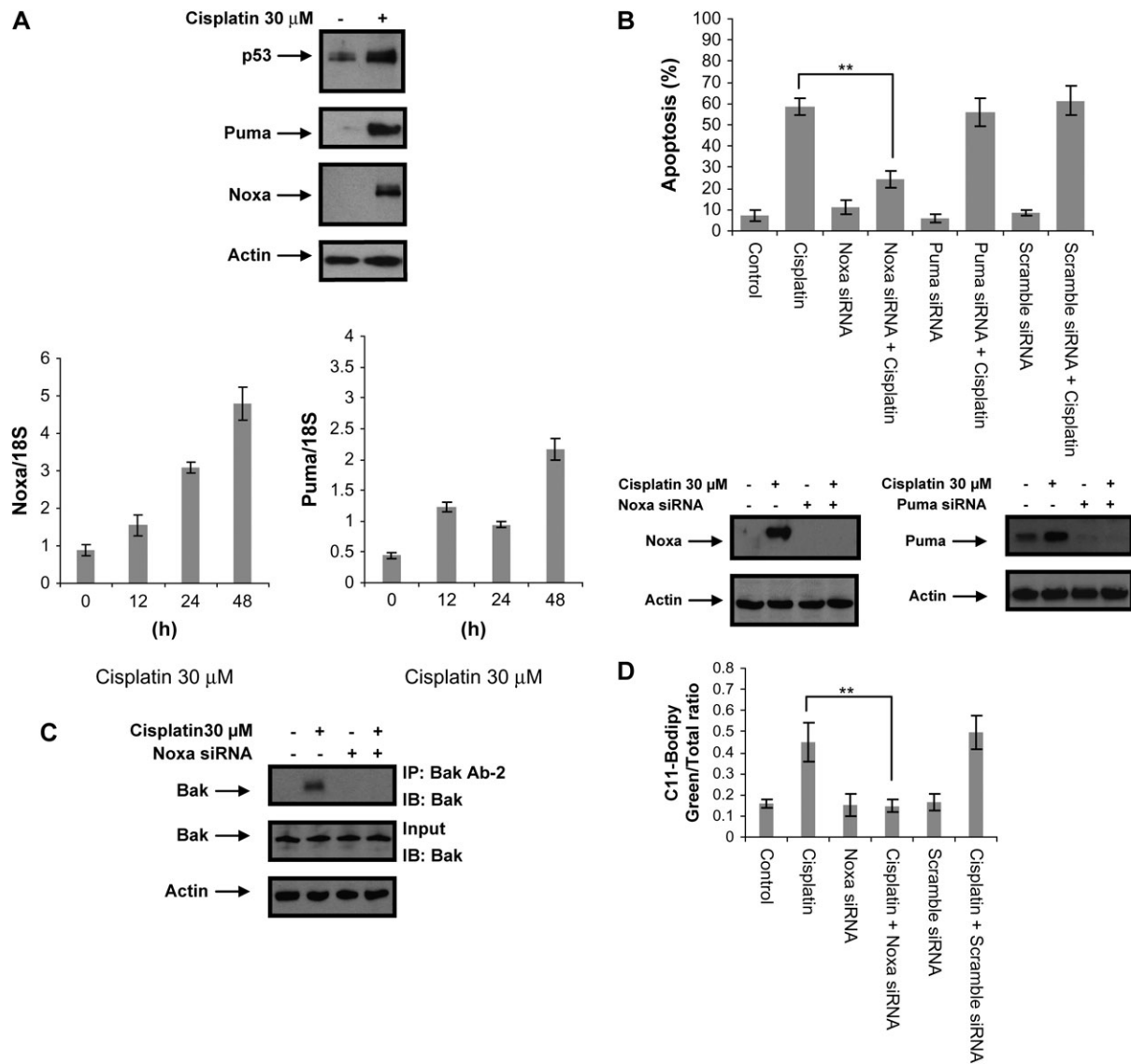

Fig. 4. Noxa mediates cisplatin-induced apoptosis in MCF-7 Bcl-2 cells. (**A**) Immunoblot analysis of p53, Puma and Noxa in untreated and cisplatin-treated (30 μM) MCF-7 Bcl-2 cells for 48 h. Actin was probed as a loading control. Noxa and Puma mRNA levels were analyzed by quantitative PCR in untreated and cisplatin-treated (30 μM) MCF-7 Bcl-2 cells for 48 h. Results were normalized to the 18 S ribosomal RNA. (**B**) MCF-7 Bcl-2 cells were treated with Noxa siRNA, Puma siRNA or scramble siRNA for 48 h and exposed to cisplatin (30 μM) for 48 h. Apoptosis was assessed by flow cytometric analysis after Annexin V staining. Total cell lysates were analyzed by immunoblot for Noxa and Puma to verify the effectiveness of Noxa siRNA and Puma siRNA. Actin was used as a loading control. Columns, mean of three independent experiments; bars, standard error. $^{**}P < 0.01$, cisplatin-treated compared with cisplatin plus Noxa siRNA-treated cells. (**C**) MCF-7 Bcl-2 cells were treated with Noxa siRNA and exposed to cisplatin (30 μM) for 36 h. Activation of Bak was explored by immunoprecipitation using active conformation-specific anti-Bak (Ab-2) antibody followed by immunoblot analysis. Five percent of the input for immunoprecipitation was also subjected to immunoblot analysis. Actin was used as a loading control. (**D**) MCF-7 Bcl-2 cells were transfected with Noxa siRNA or scramble siRNA. Cells were treated with cisplatin (30 μM) for 48 h and lipid peroxidation was assessed by C11-BODIPY (581/591) fluorescence probe. Data were shown as C11-BODIPY Green/Total fluorescence ratio. Columns, mean of three independent experiments; bars, standard error. $^{**}P < 0.01$, cisplatin-treated compared with cisplatin plus Noxa siRNA-treated cells.

Moreover, quantitative real-time PCR analysis demonstrated that Noxa and Puma mRNA levels increased in MCF-7 Bcl-2 cells treated with cisplatin suggesting transactivation of both genes (Figure 4A). To test whether cisplatin-induced apoptosis is mediated by upregulation of Noxa or Puma, MCF-7 Bcl-2 cells were transfected with Noxa siRNA, Puma siRNA or scramble siRNA. The efficiency of siRNA-mediated knockdown was verified by monitoring Noxa and Puma protein levels using immunoblot analysis (Figure 4B). As demonstrated in Figure 4B, cisplatin-induced apoptosis was significantly decreased in Noxa siRNA-treated MCF-7 Bcl-2 cells, whereas Puma siRNA or scramble siRNA had no effect on cisplatin-induced apoptosis. On the other hand, transfection of cells with Noxa, Puma or scramble siRNA alone did not affect apoptotic response. M30 Apoptosense ELISA experiments further confirmed that knockdown of Noxa impaired cisplatin-induced apoptotic response in MCF-7 Bcl-2 cells (supplementary Figure S5A is available at *Carcinogenesis* Online). In addition, knockdown of Noxa by siRNA also decreased cisplatin-induced MMP loss and caspase-9 activation in MCF-7 Bcl-2 cells (supplementary Figure S5B and C are available at *Carcinogenesis* Online). Next, we sought to determine whether Bak activation by cisplatin in MCF-7 Bcl-2 cells was dependent on Noxa induction. Bak was immunoprecipitated with the active conformation antibody in untreated, cisplatin-treated, Noxa siRNA-treated or cisplatin plus Noxa siRNA-treated MCF-7 Bcl-2 cells and active Bak was detected by means of immunoblot. Knockdown of Noxa by siRNA completely blocked cisplatin-triggered Bak activation in MCF-7 Bcl-2 cells (Figure 4C). Since lipid peroxidation was required for induction of apoptosis by cisplatin in MCF-7 Bcl-2 cells, we evaluated whether siRNA-mediated knockdown of Noxa has any effect on cisplatin-induced lipid peroxidation using C11-Bodipy (581/591) fluorescence probe. Treatment with Noxa siRNA dramatically attenuated cisplatin-induced lipid peroxidation in MCF-7 Bcl-2 cells (Figure 4D), which suggests that formation of lipid peroxidation end products by cisplatin is downstream of Noxa induction.

p53 transactivation is involved in cisplatin-induced apoptosis

To evaluate the involvement of p53 pathway cisplatin-induced apoptosis, MCF-7 Bcl-2 cells were transfected with either pCMV vector (Vector) or dominant-negative p53 mutant p53DD. The expression of p53 and p53DD was confirmed by immunoblot analysis (Figure 5A). Cells were treated with cisplatin for 48 h and apoptotic response was evaluated by Annexin V assay. As shown in Figure 5B, expression of p53DD clearly decreased cisplatin-induced apoptosis in MCF-7 Bcl-2 cells, while cisplatin successfully activated apoptosis in untransfected or vector-transfected cells. Transfection with vector or p53DD alone did not alter the apoptotic response. As an alternative approach, we utilized siRNA-mediated knockdown of p53 in MCF-7
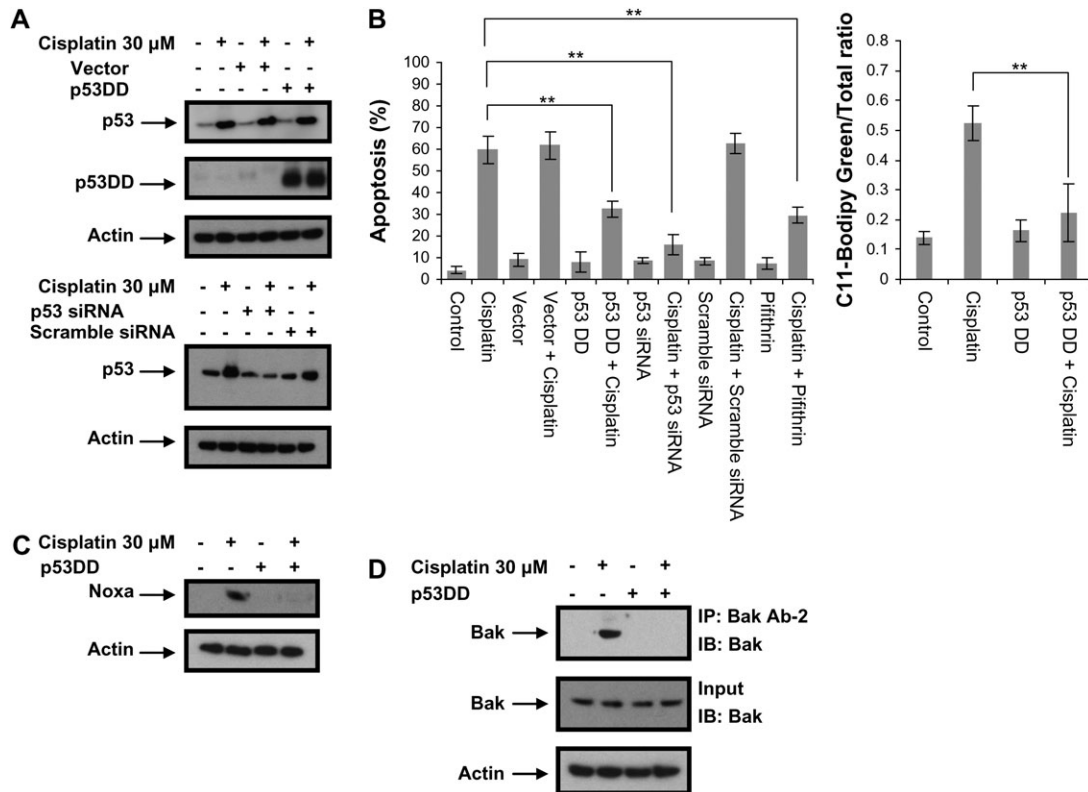
Fig. 5. p53 activity is required for cisplatin-induced apoptosis in MCF-7 Bcl-2 cells. (**A**) MCF-7 Bcl-2 cells were transfected either with pCMV empty vector (Vector) or with pCMV-p53DD (dominant-negative p53 mutant). Cells were treated with cisplatin for 48 h and the expression of p53 (using anti-p53 DO-1; Santa Cruz) and 14 kDa p53DD (using anti-p53 pAB421; Calbiochem) was verified by immunoblot analysis (top). MCF-7 Bcl-2 cells were treated with p53 siRNA or scramble siRNA for 48 h and treated with cisplatin (30 μM) for 48 h. Knockdown of p53 was determined by immunoblot analysis (bottom). (**B**) pCMV empty vector (Vector)-transfected, p53DD-transfected, p53 siRNA-transfected, scramble siRNA-transfected or pifithrin-α-treated (20 μM) MCF-7 Bcl-2 cells were exposed to cisplatin (30 μM) for 48 h and apoptotic response was evaluated by Annexin V staining and flow cytometry. Columns, mean of three independent experiments; bars, standard error. **$P < 0.01$, cisplatin-treated compared with cisplatin-treated plus p53DD-transfected cells, cisplatin plus p53 siRNA-treated cells and cisplatin plus pifithrin-α-treated cells. p53DD-transfected or untransfected MCF-7 Bcl-2 cells were treated with cisplatin (30 μM) for 48 h and lipid peroxidation was assessed by C$_{11}$-BODIPY (581/591) fluorescence probe. Data are shown as C$_{11}$-BODIPY Green/Total fluorescence ratio. Columns, mean of three independent experiments; bars, standard error. **$P < 0.01$, cisplatin-treated compared with cisplatin-treated plus p53DD-transfected cells. (**C**) MCF-7 Bcl-2 cells were transfected with pCMV-p53DD and treated with cisplatin for 48 h. Noxa protein levels were detected by immunoblot analysis. Actin was probed as a loading control. (**D**) MCF-7 Bcl-2 cells were transfected with pCMV-p53DD and treated with cisplatin for 36 h. Activation of Bak was explored by immunoprecipitation using active conformation-specific anti-Bak (Ab-2) antibody followed by immunoblot analysis. Five percent of the input for immunoprecipitation was also subjected to immunoblot analysis. Actin was used as a loading control.

Bcl-2 cells to examine the contribution of p53 in cisplatin-induced apoptosis. We transfected MCF-7 Bcl-2 cells with either p53 siRNA or scramble siRNA and treated with cisplatin for 48 h. Knockdown of p53 by siRNA-mediated silencing was determined by immunoblot analysis of untreated or cisplatin-treated cells (78% efficiency by densitometric analysis when normalized for actin, cisplatin treated compared with cisplatin plus p53 siRNA-treated cells) (Figure 5A). As shown in Figure 5B, p53 siRNA significantly inhibited apoptosis promoted by cisplatin in MCF-7 Bcl-2 cells, while scramble siRNA did not have a similar effect. In addition, transfection with p53 siRNA or scramble siRNA alone did not have any significant effect. Furthermore, pretreating MCF-7 Bcl-2 cells with a small-molecule inhibitor of p53 transcriptional activity, pifithrin-α, decreased cisplatin-triggered apoptotic response (Figure 5B). Pifithrin-α treatment alone had no effect on apoptotic response of MCF-7 Bcl-2 cells. Expression of p53DD in MCF-7 Bcl-2 cells decreased cisplatin-induced lipid peroxidation, which underscores the important role of p53 transcriptional activity for cisplatin-induced lipid peroxidation. Moreover, expression of p53DD decreased Noxa induction by cisplatin in MCF-7 Bcl-2 cells (Figure 5C). These findings indicate that p53 transcriptional activity is required for cisplatin-induced upregulation of Noxa and apoptosis of MCF-7 Bcl-2 cells.

Next, we explored whether p53 is functioning upstream of Bak activation upon cisplatin treatment in MCF-7 Bcl-2 cells. Immunoprecipitation analysis with active conformation-specific Bak antibody demonstrated that transfection of MCF-7 Bcl-2 cells with dominant-negative p53DD impaired cisplatin-induced Bak activation (Figure 5D). Together, these data suggest that p53 acts upstream of Bak activation to promote cisplatin-mediated activation of apoptotic machinery through induction of Noxa.

Cisplatin promotes Noxa–Mcl-1 and p53–Bcl-x_L interactions

In Figure 6A, we demonstrated that Noxa complexed to Mcl-1 dramatically increased following cisplatin treatment in MCF-7 Bcl-2 cells, whereas Bak–Mcl-1 interaction was disrupted. Reciprocal coimmunoprecipitation experiments also revealed that cisplatin induced an increased Noxa–Mcl-1 interaction in parallel to increased Noxa protein levels (Figure 6A). However, we did not detect any Mcl-1–Bax or Mcl-1–p53 interaction. We observed increased Bcl-x_L–p53 interaction in cisplatin-treated cells, which was confirmed by reciprocal coimmunoprecipitation (Figure 6B). We could not detect any Bcl-x_L–Noxa, Bcl-x_L–Bax or Bak–Bcl-x_L interaction in MCF-7 Bcl-2 cells. These results suggest that p53 mediates cisplatin-induced apoptosis in MCF-7 Bcl-2 cells via two concomitantly engaged mechanisms: (i) by increasing Noxa levels to inhibit Mcl-1 antiapoptotic function via transcriptional activation and (ii) by directly binding and blocking Bcl-x_L antiapoptotic function. In MCF-7 Bcl-2 cells, we found that Bcl-2 did not interact with Noxa, Bax, Bak or p53 in untreated or cisplatin-treated cells (Figure 6C). A summary of these mechanisms is presented in Figure 6D.

Discussion

Mitochondrial apoptotic signaling is mainly governed by Bcl-2 protein family members. Antiapoptotic Bcl-2 proteins have been shown to inhibit apoptosis induced by various stimuli including chemotherapeutics (1–5,7). p53 is an important tumor suppressor gene, but the involvement of p53 in mitochondrial apoptosis signaling remains to be identified. Our results in this study show that cisplatin activates a proapoptotic pathway that bypasses Bcl-2-mediated protection against apoptosis in Bcl-2-overexpressing MCF-7 cells, accompanied by the release of cytochrome *c* into cytosol, loss of MMP and activation of caspases (Figure 1; supplementary Figure 1 is available at *Carcinogenesis* Online). Previous work has suggested that cisplatin might induce cell death via mechanisms other than apoptosis (39,40), but our results clearly indicate that the mode of cell death triggered by cisplatin in MCF-7 Bcl-2 cells is mitochondrial apoptosis.

Considering the finding that cisplatin induced apoptosis in both parental MCF-7 (p53 wild-type) and MDA-MB-231 (p53 mutated) cell lines, we can conclude that apoptosis induction by cisplatin does not require p53 transcriptional activity in parental breast cancer cells consistent with a previous report (41). Interestingly, cisplatin did not lead to apoptosis in MDA-MB-231 cells overexpressing Bcl-2. Thus, proapoptotic mechanisms which were activated by cisplatin in MDA-MB-231 cells could be successfully decreased by Bcl-2. We conclude that this differential response in MCF-7 Bcl-2 and MDA-MB-231 Bcl-2 cells may be related to selective activation of p53 proapoptotic pathway in MCF-7 Bcl-2 cells.

Our results show that selective activation of Bak is a key event for the promotion of mitochondrial membrane permeabilization by cisplatin in MCF-7 Bcl-2 cells. Independent action of Bak and Bax has been shown in other systems, e.g. in primary baby mouse kidney epithelial cells, Bax and Bak were shown to independently mediate tumor necrosis factor-α-mediated apoptosis (42). Also, enforced expression of p14^{ARF} in osteosarcoma and colon cancer cell lines triggered apoptosis through activation of a Bax-independent apoptotic pathway (43), and Bak-deficient Jurkat T leukemia cells were demonstrated to be resistant to apoptosis triggered by ultraviolet or anticancer drugs (44). It has been shown that expression of antisense Bak in MCF-7 cells renders them more resistant to cisplatin and that cisplatin preferentially activates Bak in cisplatin-sensitive melanoma cell lines (45,46). In addition, MCF-7 cells expressing green fluorescent protein-Bak were also shown to be more sensitive to apoptosis induced by staurosporine, actinomycin D, TRAIL and Puma overexpression (47). These results argue that the Bak-mediated mitochondrial apoptotic pathway is a promising target even in cells with compromised Bax function.

Puma and Noxa are two important proapoptotic BH3-only proteins and transcriptional targets of p53-mediated apoptosis signaling, although p53-independent induction of Puma and Noxa has been reported (48–52). Here, we demonstrated the critical involvement of Noxa, but not Puma, upstream of Bak activation and mitochondrial membrane permeabilization in cisplatin-induced apoptosis in MCF-7 Bcl-2 cells. Induction of Noxa was p53 dependent and absolutely required for cisplatin-induced apoptosis in Bcl-2-overexpressing MCF-7 cells. The protein–protein interaction patterns of Bcl-2 proteins are hierarchically regulated (9,11). It was shown previously that Noxa selectively engages Mcl-1 and does not interact with Bcl-2 or Bcl-x_L (11,53). We utilized coimmunoprecipitation analysis to identify the interaction pattern of Noxa with antiapoptotic Bcl-2 proteins, which indicated Noxa–Mcl-1 interaction following cisplatin treatment in MCF-7 Bcl-2 cells. Concordantly, Mcl-1-bound Bak was displaced by Noxa to promote apoptosis. In contrast, Noxa did not interact with Bcl-x_L or Bcl-2 in untreated or cisplatin-treated cells.

Of note, activation of apoptosis by cisplatin in MCF-7 Bcl-2 cells occurred at a fairly late time point compared with parental MCF-7 cells, which suggests a gradual engagement of the proapoptotic machinery to overcome Bcl-2-mediated antiapoptotic potency. In contrast, two other drugs with distinct modes of action, paclitaxel and HA14-1, failed to exert a similar effect both in MCF-7 Bcl-2 and MDA-MB-231 Bcl-2 cell lines. This gradual development of apoptosis is consistent with a gradual buildup of lipid peroxidation effects, as indicated by our present findings. Both ROS and lipid peroxidation have been reported to mediate cisplatin-induced apoptosis in various cancer cell types (19,54). Previous studies revealed the protective function of Bcl-2 against ROS production and lipid peroxidation (15–17), but the mechanism by which Bcl-2 exerts these effects is not clearly understood. Intriguingly, both knockdown and overexpression of Bcl-2 led to increased lipid peroxidation levels at 48 h compared with cells at 24 h. In both parental MCF-7 cells and MCF-7 Bcl-2 cells, cisplatin treatment resulted in increased (4-HNE)-histidine adducts in Bcl-2 protein, which suggested that lipid peroxidation end products might directly modify Bcl-2. Moreover, we observed substantial amount of (4-HNE)-histidine adducts in Bcl-2 protein in untreated MCF-7 Bcl-2 cells, which may explain the increased level of peroxidation in Bcl-2-overexpressing cells.
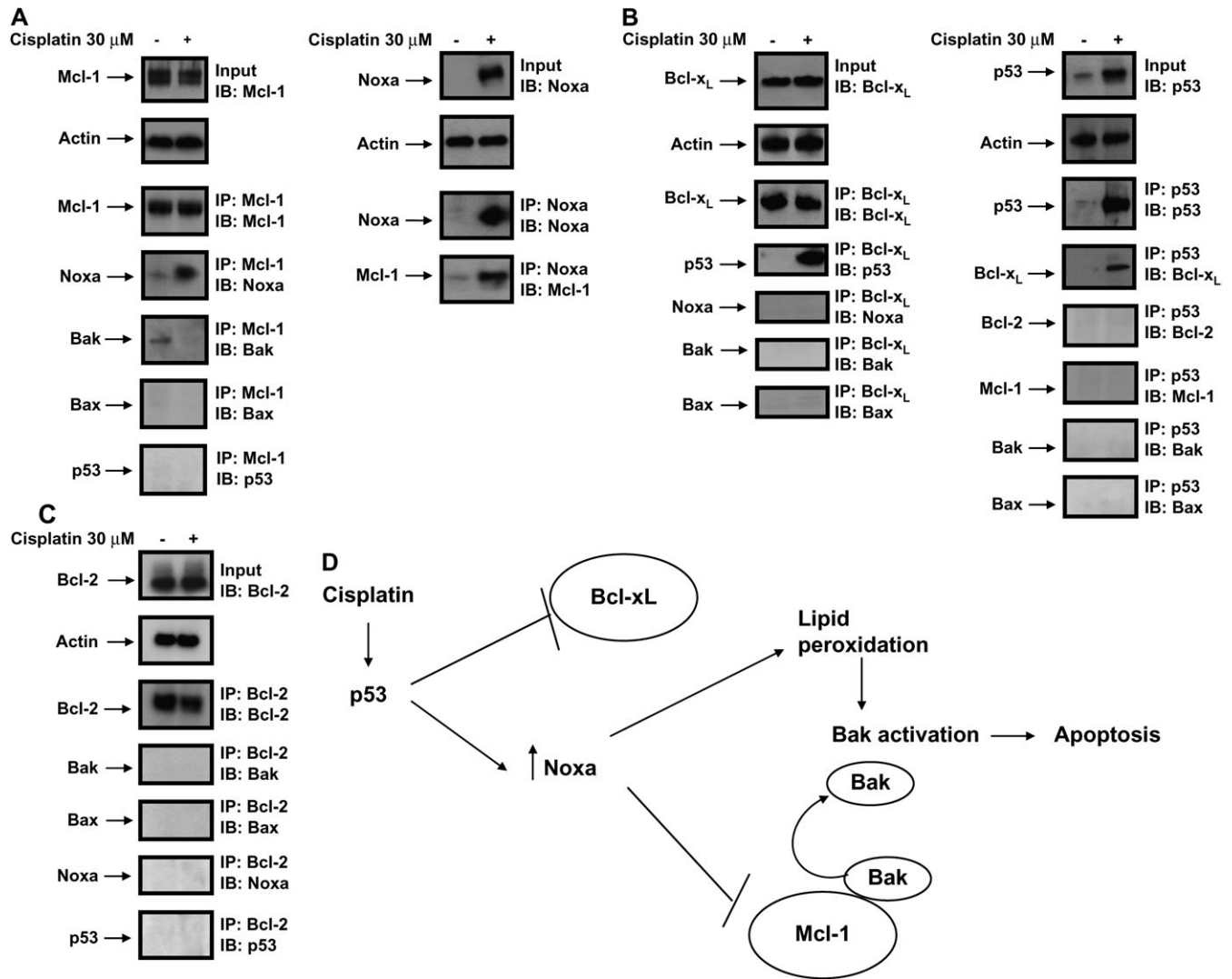
Fig. 6. Cisplatin treatment induces Noxa–Mcl-1 and p53–Bcl-x$_L$ interactions and results in disruption of Bak–Mcl-1 complex. (**A**) MCF-7 Bcl-2 cells were exposed to cisplatin (30 μM) and total cell lysates were subjected to immunoprecipitation using anti-Mcl-1 antibody. Immunoprecipitates were probed for Mcl-1, Noxa, Bak, Bax and p53. Reciprocal immunoprecipitations were performed by anti-Noxa antibody and blotted for Noxa and Mcl-1. Five percent of the input for immunoprecipitation was also analyzed by immunoblot. Actin was used as a loading control. (**B**) MCF-7 Bcl-2 cells were treated with cisplatin (30 μM) and total cell lysates were analyzed by immunoprecipitation using anti-Bcl-x$_L$ antibody. Immunoprecipitates were probed for Bcl-x$_L$, p53, Noxa, Bax and Bak. Reciprocal immunoprecipitations were performed by anti-p53 antibody and blotted for p53, Bcl-x$_L$, Bcl-2, Mcl-1, Bax and Bak. Five percent of the input for immunoprecipitation was also analyzed by immunoblot. Actin was used as a loading control. (**C**) MCF-7 Bcl-2 cells were treated with cisplatin (30 μM) and total cell lysates were analyzed by immunoprecipitation using anti-Bcl-2 antibody. Immunoprecipitates were probed for Bcl-2, p53, Noxa, Bax and Bak. Five percent of the input for immunoprecipitation was also analyzed by immunoblot. Actin was used as a loading control. (**D**) Scheme for cisplatin-mediated apoptotic pathways in Bcl-2-overexpressing MCF-7 cells. Upon cisplatin treatment, p53 is activated and induces Noxa upregulation transcriptionally. Noxa induction is accompanied by enhanced Noxa–Mcl-1 interaction, disruption of Bak–Mcl-1 complexes and increased lipid peroxidation. In parallel, p53 binds to Bcl-x$_L$ and represses its antiapoptotic function, suggesting a transcription-independent proapoptotic role for p53 to promote Bak activation and apoptosis.

Increased lipid peroxidation at 48 h in Bcl-2 siRNA-treated MCF-7 cells may be due to increased targeting of other proteins and membranous structures by lipid peroxidation end products as a result of decreased Bcl-2 levels, but the exact mechanism of this observation merits further investigation.

Lipid peroxidation end products were also involved in cisplatin-induced apoptosis downstream of Noxa induction in MCF-7 Bcl-2 cells. Similarly, cisplatin-induced lipid peroxidation was inhibited by enforced expression of a dominant-negative form of p53 (p53DD). On the other hand, treatment of parental MCF-7 cells with cisplatin resulted in induction of ROS formation at 24 h and lipid peroxidation at 24 and 48 h. In addition, treatment of MCF-7 cells with antioxidants and lipid peroxidation inhibitors decreased cisplatin-induced cell death, which indicates the critical role of ROS production and lipid peroxidation in cisplatin-induced cell death.

In a recent report, acute apoptosis induced by cisplatin was shown to be mediated by ROS without involvement of nuclear DNA damage response (55). A yet-to-be-defined mechanism is how lipid peroxidation end products contribute Noxa-mediated proapoptotic pathway. Given that lipid peroxidation acts downstream of Noxa induction as confirmed by siRNA-mediated silencing of Noxa, it may be possible that generation of lipid peroxidation is required for Bak activation, oligomerization and mitochondrial membrane permeabilization.

Of interest, p53 was shown previously to translocate to mitochondria to facilitate apoptosis through interaction with antiapoptotic or proapoptotic Bcl-2 proteins (23–27). Consistent with our findings, p53 was found to interact with Bcl-x$_L$ to promote apoptosis in cooperation with Puma (26). Mitochondrial targeting of p53 has been demonstrated to exert tumor suppressor effect *in vivo* in Eμ-myc transgenic lymphoma model (25). It is reasonable to assume

O.Kutuk *et al.*

that the interaction of p53 with Bcl-x$_L$ directly contributes to cisplatin-induced apoptosis of MCF-7 Bcl-2 cells by neutralizing the binding cleft of Bcl-x$_L$ and thereby facilitating a Bak-dependent apoptotic pathway. In fact, p53 appears to act as an activator BH3-only protein in intact cells as well as in isolated mitochondria, leading to mitochondrial outer membrane permeabilization and release of cytochrome *c* (26). Consequently, the cytoplasmic (transcription independent) proapoptotic role of p53 in parallel to its transcriptional activity in nucleus seems to be critical for cisplatin-induced apoptosis, perhaps particularly in cells with high antiapoptotic potency due to overexpression of Bcl-2.

In summary, our results indicate three important findings. First, cisplatin treatment may overcome Bcl-2-mediated antiapoptotic protection. Second, this effect of cisplatin requires an intact p53 proapoptotic pathway, at both cytoplasmic/mitochondrial and nuclear levels. Third, this effect also involves lipid peroxidation. These insights may be useful for the development of novel treatment of cancer cells overexpressing antiapoptotic Bcl-2 proteins.

Supplementary material

Supplementary Figures S1–5 can be found at http://carcin.oxfordjournals.org/

References

1. Taylor,K. *et al.* (2006) Recent advances in targeting regulators of apoptosis in cancer cells for therapeutic gain. *Expert Opin. Investig. Drugs*, **15**, 669–690.
2. Woo,K.J. *et al.* (2005) Bcl-2 attenuates anticancer agents-induced apoptosis by sustained activation of Akt/protein kinase B in U937 cells. *Apoptosis*, **10**, 1333–1343.
3. Letai,A. *et al.* (2004) Antiapoptotic BCL-2 is required for maintenance of a model leukemia. *Cancer Cell*, **6**, 241–249.
4. Niizuma,H. *et al.* (2006) Bcl-2 is a key regulator for the retinoic acid-induced apoptotic cell death in neuroblastoma. *Oncogene*, **25**, 5046–5055.
5. Knezevic,D. *et al.* (2007) Bcl-2 is the target of a UV-inducible apoptosis switch and a node for UV signaling. *Proc. Natl Acad. Sci. USA*, **104**, 11286–11291.
6. Green,D.R. *et al.* (1998) Mitochondria and apoptosis. *Science*, **281**, 1309–1312.
7. Letai,A.G. (2008) Diagnosing and exploiting cancer's addiction to blocks in apoptosis. *Nat. Rev. Cancer*, **8**, 121–132.
8. Cheng,E.H. *et al.* (2001) BCL-2, BCL-X(L) sequester BH3 domain-only molecules preventing BAX- and BAK-mediated mitochondrial apoptosis. *Mol. Cell*, **8**, 705–711.
9. Letai,A. *et al.* (2002) Distinct BH3 domains either sensitize or activate mitochondrial apoptosis, serving as prototype cancer therapeutics. *Cancer Cell*, **2**, 183–192.
10. Willis,S.N. *et al.* (2005) Proapoptotic Bak is sequestered by Mcl-1 and Bcl-xL, but not Bcl-2, until displaced by BH3-only proteins. *Genes Dev.*, **19**, 1294–1305.
11. Kim,H. *et al.* (2006) Hierarchical regulation of mitochondrion-dependent apoptosis by BCL-2 subfamilies. *Nat. Cell Biol.*, **8**, 1348–1358.
12. Negre-Salvayre,A. *et al.* (2008) Advanced lipid peroxidation end products in oxidative damage to proteins. Potential role in diseases and therapeutic prospects for the inhibitors. *Br. J. Pharmacol.*, **153**, 6–20.
13. Chan,W.H. *et al.* (2007) Apoptotic signaling in methylglyoxal-treated human osteoblasts involves oxidative stress, c-Jun N-terminal kinase, caspase-3, and p21-activated kinase 2. *J. Cell. Biochem.*, **100**, 1056–1069.
14. Fukunaga,M. *et al.* (2005) Methylglyoxal induces apoptosis through oxidative stress-mediated activation of p38 mitogen-activated protein kinase in rat Schwann cells. *Ann. N. Y. Acad. Sci.*, **1043**, 151–157.
15. Amstad,P.A. *et al.* (2001) BCL-2 is involved in preventing oxidant-induced cell death and in decreasing oxygen radical production. *Redox Rep.*, **6**, 351–362.
16. Hockenbery,D.M. *et al.* (1993) Bcl-2 functions in an antioxidant pathway to prevent apoptosis. *Cell*, **75**, 241–251.
17. Bruce-Keller,A.J. *et al.* (1998) Bcl-2 protects isolated plasma and mitochondrial membranes against lipid peroxidation induced by hydrogen peroxide and amyloid beta-peptide. *J. Neurochem.*, **70**, 31–39.
18. Zamble,D.B. *et al.* (1998) p53-Dependent and -independent responses to cisplatin in mouse testicular teratocarcinoma cells. *Proc. Natl Acad. Sci. USA*, **95**, 6163–6168.
19. Bragado,P. *et al.* (2007) Apoptosis by cisplatin requires p53 mediated p38alpha MAPK activation through ROS generation. *Apoptosis*, **12**, 1733–1742.
20. Moreno,C.S. *et al.* (2007) Evidence that p53-mediated cell-cycle-arrest inhibits chemotherapeutic treatment of ovarian carcinomas. *PLoS ONE*, **2**, e441.
21. Petit,T. *et al.* (2003) p53-independent response to cisplatin and oxaliplatin in MMTV-ras mouse salivary tumors. *Mol. Cancer Ther.*, **2**, 165–171.
22. Wang,X. *et al.* (1999) Cisplatin-induced p53-independent growth arrest and cell death in cancer cells. *Int. J. Oncol.*, **15**, 1097–1102.
23. Erster,S. *et al.* (2004) *In vivo* mitochondrial p53 translocation triggers a rapid first wave of cell death in response to DNA damage that can precede p53 target gene activation. *Mol. Cell. Biol.*, **24**, 6728–6741.
24. Mihara,M. *et al.* (2003) p53 has a direct apoptogenic role at the mitochondria. *Mol. Cell*, **11**, 577–590.
25. Talos,F. *et al.* (2005) Mitochondrially targeted p53 has tumor suppressor activities *in vivo*. *Cancer Res.*, **65**, 9971–9981.
26. Chipuk,J.E. *et al.* (2005) PUMA couples the nuclear and cytoplasmic proapoptotic function of p53. *Science*, **309**, 1732–1735.
27. Leu,J.I. *et al.* (2004) Mitochondrial p53 activates Bak and causes disruption of a Bak-Mcl1 complex. *Nat. Cell Biol.*, **6**, 443–450.
28. Yamamoto,K. *et al.* (1999) BCL-2 is phosphorylated and inactivated by an ASK1/Jun N-terminal protein kinase pathway normally activated at G(2)/M. *Mol. Cell. Biol.*, **19**, 8469–8478.
29. Shaulian,E. *et al.* (1992) Identification of a minimal transforming domain of p53: negative dominance through abrogation of sequence-specific DNA binding. *Mol. Cell. Biol.*, **12**, 5581–5592.
30. Hagg,M. *et al.* (2002) A novel high-through-put assay for screening of proapoptotic drugs. *Invest. New Drugs*, **20**, 253–259.
31. Wang,H. *et al.* (1999) Quantifying cellular oxidative stress by dichlorofluorescein assay using microplate reader. *Free Radic. Biol. Med.*, **27**, 612–616.
32. Hussain,S.M. *et al.* (2002) Cellular toxicity of hydrazine in primary rat hepatocytes. *Toxicol. Sci.*, **69**, 424–432.
33. Orhan,H. *et al.* (2006) Application of lipid peroxidation and protein oxidation biomarkers for oxidative damage in mammalian cells. A comparison with two fluorescent probes. *Toxicol. In Vitro*, **20**, 1005–1013.
34. Toyokuni,S. *et al.* (1995) The monoclonal antibody specific for the 4-hydroxy-2-nonenal histidine adduct. *FEBS Lett.*, **359**, 189–191.
35. Ruiz-Vela,A. *et al.* (2005) Proapoptotic BAX and BAK control multiple initiator caspases. *EMBO Rep.*, **6**, 379–385.
36. Panaretakis,T. *et al.* (2002) Activation of Bak, Bax, and BH3-only proteins in the apoptotic response to doxorubicin. *J. Biol. Chem.*, **277**, 44317–44326.
37. Fulda,S. *et al.* (2005) Sensitization for anticancer drug-induced apoptosis by betulinic acid. *Neoplasia*, **7**, 162–170.
38. Esterbauer,H. *et al.* (1991) Chemistry and biochemistry of 4-hydroxynonenal, malonaldehyde and related aldehydes. *Free Radic. Biol. Med.*, **11**, 81–128.
39. Baek,S.M. *et al.* (2003) Differential roles of hydrogen peroxide and hydroxyl radical in cisplatin-induced cell death in renal proximal tubular epithelial cells. *J. Lab. Clin. Med.*, **142**, 178–186.
40. Vakifahmetoglu,H. *et al.* (2008) DNA damage induces two distinct modes of cell death in ovarian carcinomas. *Cell Death. Differ.*, **15**, 555–566.
41. Mandic,A. *et al.* (2003) Cisplatin induces endoplasmic reticulum stress and nucleus-independent apoptotic signaling. *J. Biol. Chem.*, **278**, 9100–9106.
42. Degenhardt,K. *et al.* (2002) Bax and Bak independently promote cytochrome C release from mitochondria. *J. Biol. Chem.*, **277**, 14127–14134.

43. Hemmati,P.G. *et al*. (2002) Adenovirus-mediated overexpression of p14(ARF) induces p53 and Bax-independent apoptosis. *Oncogene*, **21**, 3149–3161.

44. Wang,G.Q. *et al*. (2001) A role for mitochondrial Bak in apoptotic response to anticancer drugs. *J. Biol. Chem.*, **276**, 34307–34317.

45. Mandic,A. *et al*. (2001) Cisplatin induces the proapoptotic conformation of Bak in a deltaMEKK1-dependent manner. *Mol. Cell. Biol.*, **21**, 3684–3691.

46. Ihrlund,L.S. *et al*. (2006) Two distinct steps of Bak regulation during apoptotic stress signaling: different roles of MEKK1 and JNK1. *Exp. Cell Res.*, **312**, 1581–1589.

47. Neise,D. *et al*. (2008) Activation of the mitochondrial death pathway is commonly mediated by a preferential engagement of Bak. *Oncogene*, **27**, 1387–1396.

48. Nakano,K. *et al*. (2001) PUMA, a novel proapoptotic gene, is induced by p53. *Mol. Cell*, **7**, 683–694.

49. Oda,E. *et al*. (2000) Noxa, a BH3-only member of the Bcl-2 family and candidate mediator of p53-induced apoptosis. *Science*, **288**, 1053–1058.

50. Perez-Galan,P. *et al*. (2006) The proteasome inhibitor bortezomib induces apoptosis in mantle-cell lymphoma through generation of ROS and Noxa activation independent of p53 status. *Blood*, **107**, 257–264.

51. Villunger,A. *et al*. (2003) p53- and drug-induced apoptotic responses mediated by BH3-only proteins puma and noxa. *Science*, **302**, 1036–1038.

52. Wang,X. *et al*. (2006) The BH3-only protein, PUMA, is involved in oxaliplatin-induced apoptosis in colon cancer cells. *Biochem. Pharmacol.*, **71**, 1540–1550.

53. Chen,L. *et al*. (2005) Differential targeting of prosurvival Bcl-2 proteins by their BH3-only ligands allows complementary apoptotic function. *Mol. Cell*, **17**, 393–403.

54. Previati,M. *et al*. (2006) Cisplatin-induced apoptosis in human promyelo-cytic leukemia cells. *Int. J. Mol. Med.*, **18**, 511–516.

55. Berndtsson,M. *et al*. (2007) Acute apoptosis by cisplatin requires induction of reactive oxygen species but is not associated with damage to nuclear DNA. *Int. J. Cancer*, **120**, 175–180.